TITLE PAGE

Title: Removal of inhibition uncovers latent movement potential during preparation

Abbreviated title: Motor potential during saccade preparation

Authors: Uday K. Jagadisan[1,3] and Neeraj J. Gandhi[1,2,3]

Author affiliations:
[1]Department of Bioengineering
[2]Department of Neuroscience
[3]Center for the Neural Basis of Cognition
University of Pittsburgh, Pittsburgh, PA 15213

Corresponding author: Uday K. Jagadisan, Ph.D.
153 Eye and Ear Institute
203 Lothrop St
Pittsburgh, PA 15213
USA
Tel: +1-315-4099934
E-mail: kj.udayakiran@gmail.com

Author Contributions: U.K.J and N.J.G designed the study. U.K.J. performed the experiments and analyzed the data. U.K.J and N.J.G wrote the manuscript.

Number of pages: 47

Number of figures: 7 + 2 supplementary figures

Number of words: Abstract - 209, Main text - 7455, Methods - 2365

Conflict of interest: The authors declare no competing financial interests.

Acknowledgements: The study was funded by NIH grants EY022854 and EY024831 awarded to N.J.G.

Keywords: sensorimotor, superior colliculus, eye movements, threshold, parallel processing, inhibitory gating

Abstract

The motor system prepares for movements well in advance of their execution. In the gaze control system, premotor neurons that produce a burst of activity for the movement are also active leading up to the saccade. The dynamics of preparatory neural activity have been well described by stochastic accumulator models, and variability in the accumulation dynamics has been shown to be correlated with reaction times of the eventual saccade, but it is unclear whether this activity is purely preparatory in nature or has features indicative of a hidden movement command. We explicitly tested whether preparatory neural activity in premotor neurons of the primate superior colliculus has "motor potential". We removed inhibition on the saccadic system using reflex blinks, which turn off downstream gating, and found that saccades can be initiated before underlying activity reaches levels seen under normal conditions. Accumulating low-frequency activity was predictive of eye movement dynamics tens of milliseconds in advance of the actual saccade, indicating the presence of a latent movement command. We also show that reaching threshold is *not* a necessary condition for movement initiation, contrary to the postulates of accumulation-to-threshold models. The results bring into question extant models of saccade generation and support the possibility of a concurrent representation for movement preparation and generation.

Significance Statement

How the brain plans for upcoming actions before deciding to initiate them is a central question in neuroscience. Popular theories suggest that movement planning and execution occur in serial stages, separated by a decision boundary in neural activity space (e.g., "threshold"), which needs to be crossed before the movement is executed. By removing inhibitory gating on the motor system, we show here that the activity required to initiate a saccade can be flexibly modulated. We also show that evolving activity during movement planning is a hidden motor command. The results have important implications for our understanding of how movements are generated, in addition to providing useful information for decoding movement intention based on planning-related activity.

Impact Statement

Non-invasive disinhibition of the oculomotor system shows that ongoing preparatory activity in the superior colliculus has movement-generating potential and need not rise to threshold in order to produce a saccade.

Introduction

The ability to interact with the world through movements is a hallmark of the animal kingdom. Movements are usually preceded by a period of planning, when the nervous system makes decisions about the optimal response to a stimulus and programs its execution. Such planning behavior is seen in a wide variety of species, including, insects (Fotowat and Gabbiani, 2007; Card and Dickinson, 2008), fish (Preuss et al., 2006), frogs (Nakagawa and Nishida, 2012), and mammals (Hanes and Schall, 1996; Churchland et al., 2006a). A fundamental question in sensorimotor neuroscience is how planning activity is appropriately parsed in order to prepare and execute movements.

In the primate gaze control system, premotor neurons that produce a volley of spikes to generate a movement are typically also active leading up to the movement. Build-up of low frequency activity prior to the saccade command, or its signatures, have been observed in a wide variety of brain regions involved in gaze control, including the frontal eye fields (Hanes and Schall, 1996; Gold and Shadlen, 2000), lateral intraparietal area (Platt and Glimcher, 1999), and superior colliculus (SC) (Dorris et al., 1997). Since variability in the onset and rate of accumulation of low-frequency activity is correlated with eventual saccade reaction times (Hanes and Schall, 1996; Ratcliff and Rouder, 1998; Usher and McClelland, 2001), it is thought that this activity primarily dictates *when* the movement is supposed to be initiated. However, it is unclear how (or if) downstream motor networks distinguish activity related to movement preparation from the command to execute one.

One possibility is that the activity of premotor neurons undergoes a transformation from representing preparation into movement-related commands at a discrete point in time (Thompson et al., 1996; Juan et al., 2004; Schall et al., 2011), when the activity reaches a movement initiation criterion, thereby acquiring the potential to generate a movement. Indeed, this is the basis for stochastic accumulator models of saccade initiation, in which premotor activity must reach a threshold level in order to generate the movement (Hanes and Schall, 1996; Ratcliff and Rouder, 1998; Zandbelt et al., 2014). Recent work in the skeletomotor system has also suggested that neuronal population activity undergoes a state space

transformation just prior to the movement, thus permitting movement preparation without execution (Churchland et al., 2012; Kaufman et al., 2014; Elsayed et al., 2016). These related views dictate that movement planning and execution are implemented as serial processes in the motor system. Alternatively, it is possible that neurons in sensorimotor structures represent these signals concurrently, gearing up to execute a movement in proportion to the strength of the planning activity. In other words, preparatory build-up of neural activity can multiplex higher order signals while simultaneously relaying those signals to effectors; we call this latter property the "motor potential" of preparatory activity. This idea is in fact the premise of the premotor theory of attention (Rizzolatti et al., 1987; Hoffman and Subramaniam, 1995), and represents a latent behavioral manifestation of movement preparation.

How might we test for the presence of a motor potential in low frequency preparatory activity? The following thought experiment helps illustrate one approach. Consider the activity of a premotor neuron accumulating over time. Under normal circumstances, inhibitory gating on the saccadic system is released at an internally specified time, possibly when activity crosses a purported threshold level or when the population dynamics reach the optimal subspace, thus resulting in movement generation (top row in Figure 1a). We can then infer that the high frequency burst during movement execution has motor potential if neural activity is correlated with dynamics of the ensuing movement, i.e., saccade velocity is faster when burst activity is higher, and vice versa (match gray traces between top and bottom rows in Figure 1a). Now, if inhibition was somehow removed at a prior time through an experimental manipulation instead of allowing the system its natural time course (thick red line in Figure 1b), the occurrence of an early movement would indicate that ongoing low frequency preparatory activity also possesses motor potential. Importantly, this potential can be quantified by correlating neural activity with kinematics of the eye *before* the onset of the saccade proper (pre-saccade velocity traces in Figure 1b), and comparing it to the previously estimated potential after saccade onset. Furthermore, the dynamics of activity following the manipulation would indicate whether the activity must cross a decision boundary (i.e., threshold or optimal subspace) in order to produce the movement (dashed traces in Figure 1b). This

hypothetical manipulation would therefore simultaneously shed light on both concurrent processing of preparatory signals and the criterion for movement initiation.

In this study, we used the trigeminal blink reflex to remove inhibition on the gaze control network during ongoing low-frequency activity. The omnipause neurons (OPNs) in the brainstem, which discharge at a tonic rate during fixation and are suppressed during saccades (Figure 1c, Cohen and Henn, 1972; Keller, 1974), also become quiescent during eye movements associated with blinks (Schultz et al., 2010). Previous work in our lab has shown that removal of this potent source of inhibition on the saccade burst generator with reflex blinks triggers saccades at lower-than-normal latencies (Gandhi and Bonadonna, 2005), an observation that has been used to study latent sensorimotor processing in SC (Jagadisan and Gandhi, 2016), the motor potential of a target selection signal during visual search (Katnani and Gandhi, 2013), and the dynamics of movement cancellation during saccade countermanding (Walton and Gandhi, 2006). Here, we first established that the saccade-related burst in SC has motor potential under normal conditions, by correlating the activity during the burst to saccade kinematics on individual trials. Critically, when performing the same analysis in the perturbation condition, we found that the level of preparatory activity at the time of the blink was also strongly correlated with initial dynamics of the evoked movement, *prior* to the saccade proper, suggesting that ongoing sub-threshold activity in SC also possesses motor potential. Finally, we show that although these movements were preceded by an acceleration of ongoing activity following the perturbation, it is not necessary for preparatory activity in SC to reach a threshold before a saccade is produced – neural activity just prior to saccades triggered by reflex blinks was lower at both individual neuron and population levels.

Results

In order to explicitly test whether saccade preparatory activity contains a latent movement command, we transiently disinhibited the motor system during the preparatory period in monkeys performing the

delayed saccade task. Briefly, each subject fixated on a central fixation point while a saccade target appeared in the periphery. After a random delay interval, the fixation spot disappeared, which was the cue (go cue) for the animal to make a saccade to the target. We induced reflex blinks during this preparatory epoch - after the go cue and before saccade typical reaction times. A reflex blink is a suitable perturbation because it removes inhibition on the saccadic system by turning off the OPNs and triggers gaze shifts at lower-than-normal latencies (Gandhi and Bonadonna, 2005). We first describe important aspects of the blink technique here. When induced during fixation in the absence of any other target, a reflex blink is accompanied by a blink-related eye movement (BREM) – the eyes turn nasally and downward before returning to the original fixation position in a loop-like trajectory (e.g., Rottach et al., 1998). Gaze shifts triggered by the blink in the presence of a peripheral target thus have the BREM component in addition to the saccade directed towards the target; we refer to them as blink-triggered movements or blink-triggered saccades.

Figure 2a shows example velocity profiles of the BREM (thin gray traces in the left column) and the velocity profiles and spatial trajectories of three blink-triggered movements (colored traces in left and right columns, respectively) from one session. We computed onset times of saccades embedded in blink-triggered movements using a previously used model-free approach that is agnostic to any possible interaction between the BREM and saccade components (Katnani and Gandhi, 2013). Saccade onset was determined as the time at which the movement velocity on a given trial deviated (colored circles) from the expected BREM profile distribution (thick black traces in Figure 2a; only the mean BREM trace is shown in the right panel for clarity) for that session. As seen from the example blink-triggered movements, there was considerable variation in the time at which the eye movement deviated from the BREM profile towards the saccade goal, marking saccade onset. Figure 2b shows the distribution of saccade onset times relative to blink time obtained using this approach (for more details, see Methods – movement detection). It is worth noting here that the bimodality apparent in the distribution of saccade onset times in Figure 2b likely reflects the divide between trials in which the process behind saccade initiation was already

underway by the time of the blink (delays <20 ms, to the left of the vertical black line), and trials in which the saccade was triggered *due* to disinhibition by the blink (delays >20 ms, to the right of the vertical black line). Since most analyses in this study were focused on processes occurring before saccade onset, we split the data from perturbation trials into two sets, along the aforementioned divide: blink-triggered movements with saccade onset greater than 20 ms after blink onset were used for the motor potential and accumulation rate analyses, and all blink-triggered movements were used for the threshold analysis (for more details, see Methods – inclusion criteria).

The blink perturbation triggers reduced latency, but accurate, saccades

First, as one way to assay the behavioral manifestation of motor preparation, we verified that reflex blinks during the preparatory period produced low-latency saccades. Figure 3a shows saccade reaction time (from GO cue) as a function of the time of blink across all perturbation trials (red circles). To visually compare reaction times on blink trials with those in control trials, it was necessary to include the distribution of control reaction times in this figure. To do this, we created a surrogate dataset by randomly assigning blink times to control trials, and plotted them on the same axes as blink trials in Figure 3a (blue circles). Reaction times in perturbation trials were correlated with time of blink, and were significantly lower than control reaction times (mean control reaction time = 278 ms, mean blink-triggered reaction time = 227 ms, $p = 2.2 \times 10^{-197}$, one-tailed t-test), consistent with previous observations (Gandhi and Bonadonna, 2005).

We then verified whether saccades triggered by the blink were as accurate as normal saccades, in order to eliminate any potential confounds due to differences in accuracy. We calculated saccade accuracy as the Euclidean endpoint error normalized with respect to target location (inset in Figure 3b). The distributions of relative errors for all control and blink trials are shown in Figure 3b. Blink-triggered saccade accuracy was not significantly different from control saccades (mean control accuracy = 0.136, mean blink-

194 triggered accuracy = 0.133, p = 0.3, two-tailed t-test), as reported previously (Goossens and Van Opstal,
195 2000b; Gandhi and Bonadonna, 2005). We also tested for and found no relationship between blink time
196 and saccade accuracy (Spearman's correlation = 0.04, p = 0.22). Note that the eyes are closed due to the
197 blink, so visual feedback does not contribute to endpoint accuracy. Nonetheless, we have demonstrated
198 previously that blanking the visual target during the blink-triggered movement does not compromise the
199 accuracy on perturbation trials (Gandhi and Bonadonna, 2005). The blink perturbation thus provides an
200 assay to study the question of motor potential without introducing confounding factors related to saccade
201 metrics.

202

203 *SC activity is correlated with saccade kinematics for normal saccades*

204 Next, as a crucial prerequisite for our motor potential analysis, we examined how the motor burst in SC is
205 correlated with saccade kinematics. Specifically, we computed the correlation between the trial-by-trial
206 firing rates of a neuron and the corresponding velocities. This approach to estimating motor potential is
207 illustrated in Figure 4a. Since our eventual goal was to study pre-saccade motor potential in blink-
208 triggered saccades, we used the component of velocity in the direction of the saccade goal as our
209 kinematic variable on a given trial (inset in Figure 4a, see Methods – kinematic variables, for details). The
210 choice to use projected kinematics is to maintain uniformity with analyses on blink-triggered movements
211 (see next section), but performing the analysis on the raw, unprojected kinematics for control saccades
212 yielded very similar results (Supplementary Figure 1). Further, to avoid assumptions about the efferent
213 delay between SC activity and ocular kinematics, we computed the activity-velocity correlation at various
214 potential delays between the two signals (the blue bars in Figure 4a show an example delay of 12 ms –
215 compare the similarly shaded bars in the velocity and activity panels). Figure 4b shows, for an example
216 neuron, the trial-by-trial scatter of velocities at three time points (15 ms before, at, and 15 ms after
217 saccade onset – light, medium, and dark blue circles, respectively) plotted against neural activity
218 preceding those respective velocities by 12 ms.

It is not surprising to see a lack of correlation with SC activity for pre-saccade velocities, since they are largely zero or constant, by definition, for normal saccades, because the inhibitory gating by OPNs has not been removed yet. In contrast, the strong correlation between kinematics and activity following movement onset indicates the presence of a motor potential in the saccade-related burst. We systematically explored the time course of this motor potential by computing the correlation at different time points before and during the saccade, for a range of delays between activity and kinematics. We did this for each neuron, and the population average correlation coefficients at each time point and delay are shown in the heat map in Figure 4c. To aid interpretation of this figure, the light blue asterisk in the heat map refers to the correlation computed at the time points with the corresponding asterisk in Figure 4a. Motor potential of SC activity emerged only after the onset of the saccade, and lasted throughout the movement (streak of correlation below the unity line in Figure 4c).

For each time point in the velocity signal, we also computed the activity time points at which correlation was highest, shown as the running mean (black trace) in the heat map. This provides a measure of the efferent delay at which neural activity is most effective in driving movement kinematics. Note that the black trace is roughly parallel to the unity line, suggesting that the efferent delay was consistent for the duration of the movement. To characterize this property better, we plotted optimal efferent delay, calculated as the difference between the black trace and the unity line, as a function time with respect to movement onset (Figure 4d). The mean delay during the movement was -12 ms, meaning that instantaneous saccade kinematics were best predicted by SC activity 12 ms before. This value is centered within the range of previous functional estimates of the conduction delay between SC and extra-ocular muscles (8-17 ms, Miyashita and Hikosaka, 1996). The values for the delay before saccade onset are highly variable, likely due to noise in the pre-saccade velocities, and therefore should be ignored (also note that these delays are positive and therefore non-causal). Finally, Figure 4e shows the correlation values at the -12 ms delay as a function of time. The gray region is the $\pm$ 95% confidence intervals of the population average bootstrapped (trial-shuffled) distribution of correlations (see Methods – surrogate data

and statistics). Thus, for normal trials, motor potential, in the form of correlation between neural activity and eye velocity, only manifests after the onset of the saccade proper (starting 3 ms after saccade onset, $p < 0.05$, bootstrap test).

SC preparatory activity preceding the saccade-related burst possesses motor potential

Having found a correlation between SC activity and ocular kinematics during saccades, we wanted to know whether the time course of such motor potential expands when the saccadic system is disinhibited at earlier time points. Specifically, we wanted to know whether ongoing preparatory activity contained any motor potential before its maturation into a motor command. We hypothesized that, if the low-frequency preparatory activity that precedes the high-frequency burst had motor potential, removing inhibitory gating on the system would result in a slow eye movement proportional to the level of activity before accelerating into a saccade. The rationale was that, because the downstream OPNs become quiescent during the blink, activity in SC neurons that possessed motor potential would be allowed to drive the burst generators, and subsequently, the eye muscles (see circuit diagram in Figure 1c). To test this, we computed the correlation between SC activity and eye velocity before and during blink-triggered saccades in a manner like that for control saccades (Figure 5a). It is important to note that we subtracted the BREM component from the blink-triggered saccade velocities before projecting these residuals in the direction of the saccade goal (inset in Figure 5a). This was done to prevent independent variations in BREM kinematics (unrelated to SC activity) from masking any underlying motor potential-related correlation, which we found might be the case when we performed this analysis on the raw velocities for blink-triggered saccades (Supplementary Figures 2a-b). Figure 5b shows an example scatter plot of the trial-by-trial activities versus projected residual velocities for three time points with respect to saccade onset.

We then computed the population average correlation at different time points before and after the onset of the high velocity saccade, at different efferent delays. Neural activity was highly correlated with

movement kinematics after the onset of the high velocity saccade component (after time 0 in the heat map in Figure 5c), in agreement with data from control saccades. Importantly, activity was also correlated with eye kinematics before saccade onset (time points before 0 in Figure 5c), suggesting that upstream SC activity leaked through to the eye muscles as soon as the OPNs were turned off by the blink, causing activity-related deviations in the kinematics around the BREM. The black trace in Figure 5c also shows that the estimated efferent delay was similar to that observed in control trials and consistent before and after saccade onset. This is better observed in Figure 5d (red trace) – the mean delay after saccade onset was -12 ms, equal to the mean delay before saccade onset (up to 30 ms before saccade onset). The time course of efferent delay estimates for control trials from Figure 4d is also overlaid for comparison in Figure 5d (blue trace). Figure 5e shows the correlation as a function of time during the blink-triggered movement at these mean pre- and post- saccade optimal delays (red trace), with the time course for control trials from Figure 4e overlaid for comparison (blue trace). The average correlation across the population was significant (red trace above gray distribution, $p < 0.05$, bootstrap test) starting 30 ms before onset of the saccadic component and lasting until the end of the movement, reiterating the key result of the study.

Recall that, for control saccades, it made no difference whether the motor potential was computed based on the raw velocity traces or the component of velocity in the direction of the saccade (compare Supplementary Figure 1 and Figure 4), an expected result since instantaneous eye velocity is predominantly in the direction of the saccade goal during control saccades. In contrast, for blink-triggered saccades, the motor potential was revealed only when considering kinematics in the direction of the saccade goal (Figure 5), and not with the unprojected kinematics (Supplementary Figure 2). This observation is important for two reasons. First, it ensures that the pre-saccade motor potential seen during blink-triggered saccades is not a result of misestimating saccade onset within blink-triggered movements. If the observed pre-saccade correlation resulted solely from estimating saccade onset to be later than the ground truth, i.e., it is actually a peri-saccade correlation in disguise, then it should persist even with the

raw, unprojected blink-triggered velocity residuals, and at the same efferent delay as for the peri-saccade correlation. This is because we have already seen that motor potentials exist once the saccade has started. Second, it adds support to the notion of motor potential itself: if spikes from the preparatory activity of these neurons leaked through to the muscles, you would expect them to only drive kinematics in the neurons' preferred direction (as opposed to a non-selective impact on all movements). Note that the time course of motor potential, when it exists, and estimated efferent delay, are remarkably similar across all conditions and analyses (Supplementary Figure 2d-e), including the latent pre-saccade potential seen with the projected kinematics. Put together, these observations strongly suggest pre-saccade preparatory activity indeed possesses motor potential which is revealed when the appropriate correlations between neural activity and kinematic variables are computed.

Blink-triggered saccades are evoked at lower thresholds compared to normal saccades

Next, we used the fact that blink-triggered saccades are evoked at lower latencies to test an influential model of saccade initiation – the threshold hypothesis (Hanes and Schall, 1996). We asked whether it is necessary for activity in SC intermediate layer neurons to reach a fixed activity criterion in order to generate a movement. Previous studies have estimated the threshold for individual neurons in SC and FEF by assuming a specific time at which the threshold could be reached before saccade onset or by computing the time, backwards from saccade onset, at which premotor activity starts becoming correlated with reaction time (Hanes and Schall, 1996; Paré and Hanes, 2003). Given the heterogeneity of the activity profiles of premotor neurons, we think this approach is too restrictive to obtain an unbiased estimate of the threshold, if any. Instead, we took a non-parametric approach and scanned through possible times at which a putative threshold might be reached prior to saccade onset (Jantz et al., 2013). Figure 6a shows a snippet of the average population activity, normalized by the peak trial-averaged activity during control trials for each neuron, and aligned on saccade onset for control (blue traces) and blink (red traces) trials. For each neuron in this population (n = 50), we computed the average activity in

10 ms bins slid in 10 ms increments from 50 ms before to 20 ms after saccade onset (colored windows at the bottom of Figure 6a). If activity on control trials reaches the purported threshold at any one of these times before saccade onset, a comparison with activity in blink trials at that time should reveal the existence, or lack thereof, of a fixed threshold. Figure 6b shows the activity in these bins for control trials plotted against blink trials, colored according to the bins in Figure 6a. Note that the majority of points for early time bins lie below the unity line. Activity on blink trials was significantly lower compared to control activity from 50 ms before to 10 ms after saccade onset (square points, Wilcoxon signed-rank test, comparisons in each of these windows were significant at $p = 10^{-6}$, at least). The systematic trend in the linear fits (solid lines) to these points suggests that the activity on blink trials gradually approaches that on control trials; however, the earliest time at which control activity was not different from activity in blink trials was 20 ms after saccade onset (circles, Wilcoxon signed-rank test, $p = 0.8$) – too late to be considered activity pertaining to a movement initiation threshold. Thus, activity at the population level need not reach a threshold level in order to produce a movement.

Nevertheless, we wanted to know if there exist individual neurons in the population that might obey the threshold hypothesis. For each neuron, we calculated whether activity on blink trials was higher, lower, or not significantly different from activity in control trials, at each time point from -50 before to 20 ms after saccade onset (Wilcoxon rank-sum test, comparisons in each of these windows were significant at $p = 0.001$, at least). The three traces in Figure 6c represent the proportion of neurons that showed each of those three characteristics as a function of time. As late as 10 ms before saccade onset, more than 60% of the neurons had lower activity on blink trials compared to control trials (blue trace), inconsistent with the idea of a fixed threshold. Roughly 30% of the neurons did not exhibit significant differences in activity on blink and control trials at that time point (black trace); however, this observation is insufficient to conclude that the activities in the two conditions were identical, or that it must reach a threshold. Of course, it is possible that some of these neurons belong to a class for which fixed thresholds have been observed in previous studies. Together, these results suggest that it is not necessary for premotor activity

343 in SC intermediate layers to reach a threshold level at the individual neuron or population level in order to
344 produce a movement.

345

346 *Rate of accumulation of SC activity accelerates following disinhibition by the blink*

347 Since SC neurons do not necessarily cross a fixed threshold to produce movements, as we saw above, it is
348 possible that blink-triggered saccades are initiated directly off the ongoing level of preparatory activity.
349 Alternatively, low frequency SC activity may be altered by the blink, even if the saccade is triggered at a
350 lower level compared to control trials. Therefore, we studied whether the dynamics of SC activity are
351 modulated by the blink prior to saccade initiation. Since we wanted to test for a change in dynamics
352 before the actual saccade started, we restricted our analysis to the subset of trials in which saccade onset
353 occurred at least 20 ms after blink onset. This restriction reduced our population to 38 neurons. For each
354 neuron, we estimated the rate of accumulation of activity in 20 ms windows before and after blink onset
355 with piecewise linear fits (Figure 7a, dashed red trace and solid lines). It is important to note that while
356 the evolution of premotor activity is commonly modelled as a linear process, the actual dynamics of
357 accumulation may be non-linear, causing spurious changes in linear estimates of accumulation rate over
358 time. To account for this, we created a surrogate dataset of control trials for each neuron, with blink times
359 randomly assigned from the actual distribution of blink times for that session. We then performed linear
360 accumulation fits for the control dataset as well (dashed blue trace and solid lines in Figure 7a). Changes
361 in accumulation rate on control trials following the pseudo-blink should reflect the natural evolution of
362 activity at typical blink times and provide a baseline for comparing any changes observed in blink trials.
363 Figure 7b shows a scatter plot of pre- and post- blink accumulation rates on control and blink trials. Pre-
364 blink rates were not different between the two conditions (light circles, Wilcoxon signed-rank test, $p =$
365 0.4), but post-blink rates were significantly higher on blink trials (dark circles, Wilcoxon signed-rank test,
366 $p = 2.5 \times 10^{-6}$). Next, we tested for a change in accumulation rates following the blink by calculating a
367 rate change index, defined as the difference of post- versus pre- blink rates divided by their sum, for each

condition (Figure 7c). This index was positive for most neurons, even for control trials, highlighting the natural non-linear dynamics mentioned above. The change in accumulation rate was significantly higher following the actual blink on blink trials (Wilcoxon signed-rank test, $p = 4.4 \times 10^{-6}$) compared to after the pseudo-blink on control trials. Thus, removal of inhibition seems to cause an acceleration in the dynamics of ongoing activity in the lead up to a saccade.

Discussion

In this study, we sought to uncover the dynamics of movement preparation and, specifically, test whether the low-frequency preparatory activity of SC neurons encodes movement-related signals. We first established a baseline for this question by showing that, under normal conditions, saccade-related activity in the intermediate layers of SC has "motor potential", defined as correlated variability between firing rate and saccade kinematics. Then, by disinhibiting the saccadic system much earlier than its natural time course with a reflex blink, we showed that low-frequency preparatory activity in these neurons also has a latent motor potential, indicating the presence of a hidden movement command. These results suggest that the output of higher order gaze control regions like the SC possesses motor potential during both low- and high-frequency activity, but a correlation with movement kinematics may only present itself when intermediary gating (in this case presented downstream of SC by the OPNs) between the two observables is turned off. We also found that SC activity does not necessarily have to reach a threshold at the single neuron or population level in order to initiate the saccade, contrary to the postulates of an influential model of saccade initiation – the threshold hypothesis (Hanes and Schall, 1996).

Relationship between movement preparation and execution

Studies on the neural correlates of movement generation have largely focused on the divide between preparatory and executory activity, mainly due to the substantial natural latencies between the cue to

perform a movement and its actual execution. Since variability in the properties of post-cue neural activity is correlated with eventual movement reaction times (Hanes and Schall, 1996; Churchland et al., 2006b), it is thought that this activity is purely preparatory in nature, influencing only *when* the movement is supposed to be initiated (Kaufman et al., 2016), and is devoid of the potential to generate a movement, until just before its execution. Indeed, there is some evidence that movement preparation and execution have distinct neural signatures with a well-defined boundary separating them. Studies of movement preparation in the skeletomotor system have shown that neural activity reaches an optimal subspace before undergoing dynamics that produce a limb movement (Afshar et al., 2011; Churchland et al., 2012). A related idea suggests that activity pertaining to movement preparation evolves in a region of population space that is orthogonal to the optimal subspace, and this dissociation confers neurons the ability to prepare the movement by incorporating perceptual and cognitive information without risking a premature movement (Kaufman et al., 2014; Elsayed et al., 2016). However, in the absence of perturbations to the natural time course of movement generation, or explanatory models linking them to downstream processing, it is unclear whether such neural correlates are the sole causal links to the process of initiating movements.

How do we reconcile such previous observations with the finding in this study of a latent motor potential in preparatory activity? One possibility is that the oculomotor system operates differently from the skeletomotor system. More generally, it is possible that it is necessary for population activity to be in an optimal, "movement-generating" subspace in order to release inhibition and/or effectively engage downstream pathways leading up to activation of the muscles, but once the motor system has been disinhibited by another means (e.g., the blink perturbation in this study), preparatory activity is read out as if it were a movement command. Based on the results in our study, we hypothesize that the activity is likely in the movement preparation subspace when the slow eye movement is produced after the blink perturbation, and its subsequent transition into the movement execution subspace results in a high

416 velocity movement. More studies that causally delink evolving population activity from physiological
417 gating are needed to clarify these mechanisms.

418

419 *Implications for threshold-based accumulator models*

420 The threshold hypothesis is the leading model of movement preparation and initiation in the gaze control
421 system (Hanes and Schall, 1996). Inspired by stochastic accumulator models of decision-making
422 (Carpenter and Williams, 1995; Ratcliff and Rouder, 1998), this theory posits that saccade initiation is
423 controlled by accumulation to threshold of a motor preparation signal in premotor neurons. However, it is
424 unclear whether the preparatory activity must rise to a fixed biophysical threshold at the level of
425 individual neurons or a population of neurons in order to initiate a saccade (Hanes and Schall, 1996;
426 Zandbelt et al., 2014), or whether there exists a dynamic equivalent to such a threshold (Lo and Wang,
427 2006; Cisek et al., 2009).

428 Another recent study has shown that the fixed threshold hypothesis does not hold true for most neurons in
429 SC and FEF (Jantz et al., 2013), finding that the effective threshold varies based on the task being
430 performed by the subject. However, comparison of thresholds across tasks is subject to the confound that
431 the network may be in a different overall state, thereby modulating the threshold. For instance, the
432 presence or absence of the fixation spot at the time of movement initiation, or the presence of other visual
433 stimuli or distractors, may affect how downstream neurons receiving premotor activity from the whole
434 network decode the level of activity, thus influencing the effective threshold. In our study, thresholds are
435 compared between interleaved perturbation and control trials in the *same* behavioral paradigm,
436 eliminating the effect of preset network-level confounds in the premotor circuitry within SC and upstream
437 thereof.

438 Our results show that the low-frequency preparatory activity of individual or population of SC neurons
439 does not have to transition into a high-frequency mode to trigger a movement (Figure 6a, b). If gates

downstream of the SC are removed, then reduced SC activity is sufficient to move the eyes. The effective reduction in threshold (or equivalently, non-existence of a fixed threshold) that we observe is likely due to reduced activity of the OPNs, which are a potent source of inhibition on the pathway downstream of the SC. The OPNs are inhibited by the reflex blink, and thus premotor activity needs to overcome lesser inhibition and is able to trigger movements off a lower level. It is also important to note that while there is some evidence that premotor activity in SC is attenuated when saccades are perturbed by a reflex blink (Goossens and Van Opstal, 2000a), we did not observe suppression during movements that were triggered by the blink, as seen in the firing rate profile in Figure 7a. Nevertheless, the presence of any attenuation would only strengthen the result, since the occurrence of saccades despite attenuated SC activity goes against the notion of a rigid threshold.

Related considerations

It has been hypothesized that the role of a threshold may perhaps be to arbitrate between speed and accuracy during decision making and movement planning (Heitz and Schall, 2012). Studies have provided contrasting evidence for this idea, with some suggesting a collapsing bound reflecting the urgency of a movement (Cisek et al., 2009; Thura et al., 2012), and others placing the onus of balancing speed with accuracy on non-threshold features of neural activity, such as baseline and gain (Hanks et al., 2014; Salinas et al., 2014). In our study, the accuracy of reduced latency blink-triggered movements was unaltered relative to normal saccades (Figure 3b), despite the effective reduction in threshold we observed. However, the accumulation rate increased following disinhibition by the blink, suggesting that threshold and rate may be independently modulated to achieve the requisite balance between speed and accuracy.

Studies have shown that the latencies of saccades and hand movements are reduced under experimental conditions that introduce a startling stimulus (Valls-Sole et al., 1995), present targets with predictable

464 spatial and temporal features (Paré and Munoz, 1996), or provide instructions to time the movement
465 (Haith et al., 2016). We speculate that some combination of early onset of preparatory activity, higher
466 baseline, or fast accumulation to a trial-specific threshold must be achieved before the movement is
467 triggered. In terms of the population dynamics framework discussed a couple of sections back, the
468 reduction in latency can be viewed as speeding up the transition of population signals from movement
469 preparation to movement generation subspaces. It is important to note that the dynamics of movements
470 evoked under the conditions used in these experiments are remarkably similar to control movements. In
471 our view, reduced latency blink-triggered movements are not produced by the same neural mechanisms.
472 We have reported previously that delivering an air-puff to the ear or neck does not reduce the latency of
473 saccades, thus discounting the startle stimulus explanation (Gandhi and Bonadonna, 2005; Jagadisan and
474 Gandhi, 2016). Here, we randomly interleaved blink and control trials, so preparatory signals cannot start
475 to accumulate earlier and/or faster on perturbation trials. Finally, the dynamics of blink-triggered
476 movements and control saccades are not similar. Our method thus reveals a motor potential component
477 during the preparatory period that is not disclosed in the other studies.

478

479 *The role of SC and brainstem in saccade execution*

480 Although it is well-known that the locus of activity on the SC map determines amplitude and direction of
481 the saccade vector (see Gandhi and Katnani, 2011a, for a review), it has thus far been unclear whether the
482 instantaneous firing rate of SC neurons directly drives saccade kinematics, i.e., instantaneous velocity. In
483 our view, the mini-vector model of saccade execution comes closest to specifying a direct relationship
484 between SC spiking and saccade metrics (Van Gisbergen et al., 1987; Arai et al., 1994; Goossens and Van
485 Opstal, 2006). This model proposes that each spike in SC contributes to a fixed length desired
486 displacement of the eye during the window when gating is open, and has been tested with blink
487 perturbations (Goossens and Van Opstal, 2006). But it is unclear how this translates to the motor potential
488 we observe, either before or during the saccade, since we estimate this potential from correlated

variability between SC activity and eye kinematics across trials, not within a trial. Moreover, in Figure 5, this correlation is computed between activity and residual velocity projected onto the direction of the saccade target after subtraction of the BREM template. This can cause the kinematic variable to be instantaneously negative (i.e., going away from the saccade target) on some trials, but as long as it is less negative on trials when the activity is higher, we can say that the activity has motor potential. In contrast, the mini-vector model will predict that the eye moves in fixed vector increments towards the saccade target (which happens roughly to be the optimal vector of the recorded neuron). Moreover, in the previous study, not all neurons show the fixed spike count property, and at the population level, spike counts on perturbation trials are slightly higher than on control trials. This is entirely consistent with our observation that spikes can leak through when the gating is open (leading sometimes to excess spikes as in Goossens and Van Opstal, 2006; also see Buonocore et al., 2017).

Previous work has shown that the discharge profiles of burst generator neurons in the reticular formation are a scaled version of the observed eye velocity waveforms (Cullen and Guitton, 1997). Moreover, in the presence of a perturbation - for example, when a natural blink accompanies a saccade (Gandhi and Katnani, 2011b) or when a brief torque is applied to the head during eye-head gaze shifts (Sylvestre and Cullen, 2006) - burst neuron activity is also modified to account for the observed changes in eye velocity. Given these results, we predict that the lower brainstem burst generator neurons will exhibit low frequency activity to produce the slow eye movement leaked by premature inhibition of OPNs, followed by a high frequency burst that generates the saccade.

We would like to emphasize that the observed results - preparatory motor potential, reduced threshold, accelerated activity dynamics - are most likely indirect effects of the trigeminal blink reflex, via inhibition of the OPNs, and not directly due to the reflex itself. Prior work has shown that the activity of SC neurons is not affected by the BREM produced during fixation (Goossens and Van Opstal, 2000a; Jagadisan and Gandhi, 2016). For blinks produced after the saccade target is presented, some SC neurons in fact exhibit attenuation (Goossens and Van Opstal, 2000a), although we did not see it in our dataset (and even if that

514 did happen, it is counter-intuitive to and does not explain the motor potential and acceleration of activity).
515 These observations collectively suggest that the acceleration of activity that leads to a reduced latency
516 saccade is not directly due to the trigeminal blink reflex but indirectly due to OPN inhibition.

517 In our study, we found the correlation between SC activity and eye kinematics during the saccade to be
518 maximal at a time shift of 12 ms between the two signals, providing us with an estimate of the optimal
519 efferent delay between SC and extraocular muscles. This is in line with previously estimated ranges for
520 the efferent delay (8-17 ms, Miyashita and Hikosaka, 1996). In that study, single pulse microstimulation
521 was delivered to the SC during an ongoing saccade, and the latency to deviation from normal saccade
522 kinematics provided an estimate of the time it takes for a spike in SC to reach extraocular muscles while
523 the gating in the pathway downstream of SC is open. The fact that we observe the same efferent delay
524 (i.e., 12 ms) prior to saccade onset, when the OPNs are already quiescent due to the reflex blink, fits
525 neatly within this picture and adds credibility to the notion of a latent motor potential in preparatory
526 spikes.

527

528 *Parallel implementation of the sensory-to-motor transformation*

529 An influential idea in systems neuroscience is the premotor theory of attention, which posits that spatial
530 attention is manifested by the same neural circuitry that produces movements (Rizzolatti et al., 1987).
531 Consistent with this hypothesis, studies with cleverly designed behavioral tasks have attributed low-
532 frequency build-up of activity in premotor neurons to a number of cognitive processes, including target
533 selection (Schall and Hanes, 1993; Horwitz and Newsome, 1999; McPeek and Keller, 2002; Carello and
534 Krauzlis, 2004), attention (Goldberg and Wurtz, 1972; Ignashchenkova et al., 2004; Thompson et al.,
535 2005), decision-making (Newsome et al., 1989; Gold and Shadlen, 2000; Ramakrishnan and Murthy,
536 2013), working memory (Sommer and Wurtz, 2001; Balan and Ferrera, 2003), and reward prediction
537 (Platt and Glimcher, 1999; Hikosaka et al., 2006). However, such multiplexing of cognitive signals along

538 with movement preparation and execution-related activity by premotor neurons only provides
539 circumstantial evidence in support of the premotor theory, leaving open the question of whether the low-
540 frequency activity exclusively represents cognitive and preparatory processes, devoid of the concurrent
541 ability to generate a movement (a.k.a motor potential).

542 Efforts to delineate spatial attention and movement intention by means of causal manipulations have
543 produced a mixed bag of results, with some studies supporting disjoint processing (Juan et al., 2004) and
544 others supporting concurrent processing (Moore and Armstrong, 2003; Katnani and Gandhi, 2013). The
545 strongest piece of evidence yet for concurrent processing is the observation that many of these premotor
546 neurons also discharge following the onset of a visual stimulus (Wurtz et al., 2001), which can make its
547 way down to effectors resulting in an electromyographic response, e.g., in the neck (Corneil et al., 2004).
548 Such "leakage" of decision-related activity down to the muscles has also been observed in other effectors,
549 including reaches (Corneil and Munoz, 2014; Servant et al., 2015), and even across effectors (Joo et al.,
550 2016). The discovery of a latent motor potential in the preparatory activity of SC neurons significantly
551 advances this debate by suggesting that while the low-frequency build-up may not trigger movements
552 under normal conditions, movement intention and motor programming signals are also encoded by these
553 neurons in parallel. Moreover, unlike manipulations such as microstimulation or pharmacological
554 inactivation that introduce extrinsic signals that may corrupt the natural processing of this activity
555 (Katnani and Gandhi, 2013), reflex blinks are non-invasive and are likely to provide a more veridical
556 readout of ongoing processes.

557

558 *Concluding remarks*

559 It is worthwhile to end on a note of caution. The results in this study are based on experiments performed
560 in one node, SC, in a distributed network of brain regions involved in gaze control. Traditional knowledge
561 imposes a hierarchy on the sensorimotor transformations that need to occur before a gaze shift is

generated (Wurtz et al., 2001). It is possible that sensorimotor neurons in SC, and to some extent, FEF, which project directly to the brainstem burst generator (Segraves, 1992; Rodgers et al., 2006), are more likely to exhibit signatures of a motor potential in preparatory activity compared to regions higher in the cascade. Neurons in other regions may still need to signal the initiation of a movement by reaching a threshold, optimal subspace, or other similar decision bound. Furthermore, it is known that movement initiation thresholds in SC and FEF can vary based on task context (e.g., Jantz et al., 2013). The results presented here are based on a relatively simple task – the delayed saccade task. The mechanisms of movement initiation, and the presence of motor potential in preparatory activity, could in principle be different in more complex tasks, e.g. those that involve competitive spatial selection of movements or sequential movements. Future studies that take causal approaches to perturbing intrinsic population dynamics in various premotor areas across different tasks and effector modalities are essential in order to gauge whether the findings in this study point to a fundamental and generalizable property of sensorimotor systems.

584 **Methods**

585 *General and surgical procedures*

586 All experimental and surgical procedures were approved by the Institutional Animal Care and Use
587 Committee at the University of Pittsburgh and were in compliance with the US Public Health Service
588 policy on the humane care and use of laboratory animals. We used two adult rhesus monkeys (*Macaca*
589 *mulatta*, 1 male and 1 female, ages 8 and 10, respectively) for our experiments. Under isoflurane
590 anesthesia, a craniotomy that allowed access to the SC was performed and a recording chamber was
591 secured to the skull over the craniotomy. In addition, posts for head restraint and scleral search coils to
592 track gaze shifts were implanted. Post-recovery, the animal was trained to perform standard eye
593 movement tasks for a liquid reward.

594

595 *Visual stimuli and behavior*

596 Visual stimuli were displayed by back-projection onto a hemispherical dome. Stimuli were white squares
597 on a dark grey background, 4x4 pixels in size and subtended approximately 0.5° of visual angle. Eye
598 position was recorded using the scleral search coil technique, sampled at 1 kHz. Stimulus presentation
599 and the animal's behavior were under real-time control with a LabVIEW-based controller interface
600 (Bryant and Gandhi, 2005). After initial training and acclimatization, the monkeys were trained to
601 perform a delayed saccade task. The subject was required to initiate the trial by looking at a central
602 fixation target. Next, a target appeared in the periphery but the fixation point remained illuminated for a
603 variable 500-1200 ms, and the animal was required to delay saccade onset until the fixation point was
604 extinguished (GO cue). Trials in which fixation was broken before peripheral target onset were removed
605 from further analyses. The animals performed the task correctly on >95% of the trials. During each
606 session, we presented the targets in one of two locations – either inside the response field of the recorded
607 neuron, or in the diametrically opposite location (see below).

608

609 *Induction of reflex blinks*

610 On 15-20% of trials, fixation was perturbed by delivering an air puff to the animal's eye to invoke the
611 trigeminal blink reflex. Compressed air was fed through a pressure valve and air flow was monitored with
612 a flow meter. To record blinks, we taped a small Teflon-coated stainless steel coil (similar to the ones
613 used for eye tracking, but smaller in coil diameter) to the top of the eyelid. The air pressure was titrated
614 during each session to evoke a single blink. Trials in which the animal blinked excessively or did not
615 blink were excluded from further analyses. The air-puff delivery was randomly timed to evoke a blink
616 either during fixation (400-100 ms before target onset) or 100-250 ms after the GO cue, during the early
617 phase of the typical saccade reaction time. The blink evoked during fixation produced a slow and loopy
618 blink-related eye movement (BREM, gray traces in Figure 2a). The eyes returned to near the original
619 position and fixation was re-established for 400-100 ms before a target was presented in the periphery and
620 the remainder of the delayed saccade task continued. The window constraints for gaze were relaxed for a
621 period of 200-500 ms following delivery of the air puff to ensure that the excursion of the BREM did not
622 lead to an aborted trial. The blink evoked after the GO cue typically produced a blink-triggered
623 movement that can be described as a combination of a BREM and a saccade to the desired target location
624 (colored traces in Figure 2a). We used deviations from the BREM profile to determine true saccade onset,
625 as described in more detail in the next section.

626

627 *Movement detection*

628 Data were analyzed using a combination of in-house software and Matlab. Eye position signals were
629 smoothed with a phase-neutral filter and differentiated to obtain velocity traces. Normal saccades,
630 BREMs, and blink-triggered gaze shifts were detected using standard onset and offset velocity criteria (50
631 deg/s and 30 deg/s, respectively). Onsets and offsets were detected separately for horizontal and vertical

components of the movements and the minimum (maximum) of the two values was taken to be the actual onset (offset). Saccade onset times within blink-triggered movements were detected using a non-parametric approach (Katnani and Gandhi, 2013, also see Figure 2a). We first created an estimate of the expected BREM distribution during each session by computing the instantaneous mean and standard deviation of the horizontal and vertical BREM velocity profiles. Then, for each blink-triggered movement in that session, we determined the time point at which the velocity exceeded the $\pm$ 2.5 s.d. bounds of the BREM profile distribution, and remained outside those bounds for at least 15 successive time points. We did this separately for the horizontal and vertical velocity profiles, and took the earlier time point between the two components as the onset of the saccade. We further manually verified that the detected saccadic deviations on individual trials were reasonable, esp., in the spatial domain. Figure 2a illustrates this approach for three example trials.

Electrophysiology

During each recording session, a tungsten microelectrode was lowered into the SC chamber using a hydraulic microdrive. Neural activity was amplified and band-pass filtered between 200 Hz and 5 kHz and fed to a digital oscilloscope for visualization and spike discrimination. A window discriminator was used to threshold and trigger spikes online, and the corresponding spike times were recorded. The location of the electrode in the intermediate layers of SC was confirmed by the presence of visual and movement-related activity as well as the ability to evoke fixed vector saccadic eye movements at low stimulation currents (20-40 µA, 400 Hz, 100 ms). Before beginning data collection for a given neuron, its response field was roughly estimated. During data collection, the saccade target was placed either in the neuron's response field or at the diametrically opposite location (reflected across both axes) in a randomly interleaved manner. Response field centers, and therefore, target locations (also consequently, saccade amplitudes and directions) varied between 9-25 degrees in eccentricity and spanned all directions.

656

657 *Data analysis – neural pre-processing*

658 Spike density waveforms were computed for each neuron and each trial by convolving the raw spike
659 trains with a Gaussian kernel. We used a 3 ms wide kernel for the motor potential and threshold analysis
660 (involving across-trial correlations or trial-averaged neural activity) and a 10 ms kernel for the
661 accumulation rate analysis (for better rate estimation on individual trials). For a given neuron and target
662 location, spike densities were averaged across trials after aligning to target and saccade onsets. Neurons
663 were classified as visual, visuomovement or movement-related, based on the presence of a significant
664 target and/or saccade-related response. We only analyzed visuomovement and movement neurons for this
665 study, the majority of which were visuomovement (47/50). Where necessary, we normalized the trial-
666 averaged spike density of each neuron to enable meaningful averaging across the population. The activity
667 of each neuron was normalized by its peak trial-averaged firing rate during normal saccades.

668

669 *Data analysis – inclusion criteria*

670 Overall, we recorded from 64 neurons for 12339 control trials and 2364 blink trials over 50 sessions. For
671 all analyses, we only considered neurons for which we had at least 10 blink perturbation trials with the
672 target in the response field. Since we only introduced the blink perturbation on a small percentage of trials
673 in a given session in order to prevent habituation, this restricted our population to 50 neurons (7891
674 control trials and 1615 blink trials over 43 sessions). We used all 50 neurons for the threshold analysis
675 (Figure 6). For the motor potential analysis (Figure 5), since our aim was to correlate neural activity with
676 eye kinematics before saccade onset, we used only the subset of trials where the onset of the saccade was
677 delayed with respect to overall movement onset by at least 20 ms (see Figure 2b). To ensure that the
678 correlation values were reliable, we used only neurons which had at least 10 trials meeting the above
679 criterion. This restriction reduced the number of neurons available for the motor potential analyses to 38

(6771 control trials and 869 blink trials over 32 sessions), and we used the same neurons for control trials to enable meaningful comparison (Figure 4). For the same reason, we also used this subset of neurons for the accumulation rate analysis (Figure 7), where we compared the dynamics of neural activity in 20 ms windows before and after blink onset, and we wanted to ensure that the post-blink window did not include activity co-occurring with the saccade.

Kinematic variables

For the motor potential analyses in Figures 4 and 5, we computed the across-trial correlation between instantaneous movement kinematics and neural activity for each neuron. We computed the kinematic variable of relevance for each analysis as follows. In all cases, we used the raw or modified (see below) horizontal and vertical velocity signals to compute a single vectorial velocity signal using the Pythagorean theorem: $\boldsymbol{v}(t) = \sqrt{\boldsymbol{v}_h^2(t) + \boldsymbol{v}_v^2(t)}$. For the analyses in Supplementary Figure 1, for control trials, we used the raw, unmodified velocity signals to compute vectorial velocity as a function of time, which we then used as the instantaneous kinematic variable to correlate with neural activity. For perturbation trials in Figure 5 and Supplementary Figure 2, we first noted that the blink-related eye movement (BREM) contributes a substantial velocity component to the overall movement, since the initial phases of velocity and spatial profiles of blink-triggered movements look largely like those of a BREM (see Figure 2a). Thus, in order to extract only the saccadic component of a blink-triggered movement, we subtracted from it the mean BREM template on a given session, and used only the horizontal and vertical residuals to compute the vectorial residual velocity: $\tilde{v}(t) = \sqrt{\tilde{\boldsymbol{v}}_h^2(t) + \tilde{\boldsymbol{v}}_v^2(t)}$, which was used for the correlation analysis in Supplementary Figure 2.

A potential pitfall when using residual velocities by just subtracting out the mean BREM, given the variability in BREM profiles across repetitions, is that intrinsic variability of the BREM itself may mask

any correlated variability that might be present between ocular kinematics and neural activity. In other words, if the BREM is driven by an independent pathway compared to the saccade/SC activity, it represents an orthogonal source of variability in the kinematics relative to the activity-driven variability that is being examined. Therefore, for the perturbation trial analysis in Figure 5, we used the component of residual velocity in the direction of the saccade goal, to isolate variability in the direction of the saccade. The kinematic variable for this analysis is thus defined as: $\widetilde{v_\theta}(t) = \sqrt{\tilde{\boldsymbol{v}}_h^2(t) + \tilde{\boldsymbol{v}}_v^2(t)}\cos\theta$, where θ is the angle between the instantaneous residual velocity vector and the direction of the saccade goal (e.g., between the green and black vectors in the inset in Figure 5a). For the sake of consistency, we used a similar variable: $\boldsymbol{v_\theta}(t) = \sqrt{\boldsymbol{v}_h^2(t) + \boldsymbol{v}_v^2(t)}\cos\theta$, for the equivalent control analysis in Figure 4, even though the instantaneous direction of velocity is largely towards saccade goal in this condition.

Motor potential estimation

To estimate motor potential, we computed the correlation between instantaneous neural activity and eye kinematics (according to the variables defined above) across trials, across a span of efferent delays (time shifts) between activity and velocity. For each neuron, we computed the Pearson's correlation coefficient $c_{t+\Delta,t} = corr(\boldsymbol{a}(t+\Delta), \boldsymbol{v}(t))$ between the activity vector $\boldsymbol{a}(t) = [a^1(t), \dots, a^n(t)]$ and the kinematics vector $\boldsymbol{v}(t) = [v^1(t), \dots, v^n(t)]$ at time separations or lags $\Delta \in [-50,50]$, where n is the number of trials for that condition for that neuron. Each point in panel c in Figures 4-5 and Supplementary Figures 1-2 represents the average correlation coefficient across the population of neurons between firing rate and kinematics at the corresponding time points $(t, t+\Delta)$. To estimate the optimal efferent delay between activity and velocity, we computed the time at which this population average correlation peaks along the activity axis (vertical axis in the panel c heatmaps) for each time point during the movement. A moving average (5 ms window) of this efferent delay trace is shown as the black trace in the heatmaps. The

vertical distance of this trace from the unity line is equal to the the actual value of the optimal efferent delay at each movement time point, shown in panel d in Figures 4-5 and Supplementary Figures 1-2. We then calculated the mean efferent delay during the movement after saccade onset (and before saccade onset in the perturbation condition), and plotted the population average correlation at this delay (panel e in the aforementioned figures).

Surrogate data and statistics

For the accumulation rate analysis in Figure 7, we created a surrogate dataset of control trials with blink times randomly sampled from the distribution of blink occurrences in perturbation trials for that session and assigned to individual control trials. For each neuron, we created 1000 such pseudo-trials by resampling from and reassigning to control trials. We then fit the accumulation rates 20 ms before and after the blink with piecewise-linear functions. The slopes of the linear fits were taken to be the pre- and post-blink rates of accumulation for each neuron. We then compared the change in accumulation rates before and after the pseudo-blink in control trials and the blink in perturbation trials by computing the rate modulation index for each condition as $\frac{rate_{post}-rate_{pre}}{rate_{post}+rate_{pre}}$. Note that we also created a similar surrogate dataset for control trials for the purpose of visualization alone in Figure 3a.

To estimate the significance of the correlation profile in the motor potential analyses, we performed a bootstrap analysis on a trial-shuffled dataset using the motor potential estimation procedures laid out in the previous section. For each neuron, we shuffled trial identities between the across-trial activity and velocity vectors, and computed population average correlation as before. We performed this for 100 different shuffles, and the resultant across-shuffle mean correlation trace at the optimal efferent delay (as estimated from the true data) and the 95% confidence interval bounds are shown in panel e in Figures 4-5 and Supplementary Figures 1-2. At each time point, we calculated the difference between the actual correlation profile and each iteration of the bootstrap, and computed the 95% confidence interval of this

750 difference distribution. The correlation at a particular time was considered significant if this interval did
751 not contain 0. For comparisons of threshold and accumulation rate between control and blink-triggered
752 conditions, we used appropriate non-parametric statistical tests – the Wilcoxon rank sum test when
753 comparing distributions across trials, and the Wilcoxon signed-rank test for trial-averaged comparison
754 across a population.

755

756

757

758

759

760

761

762

763

764

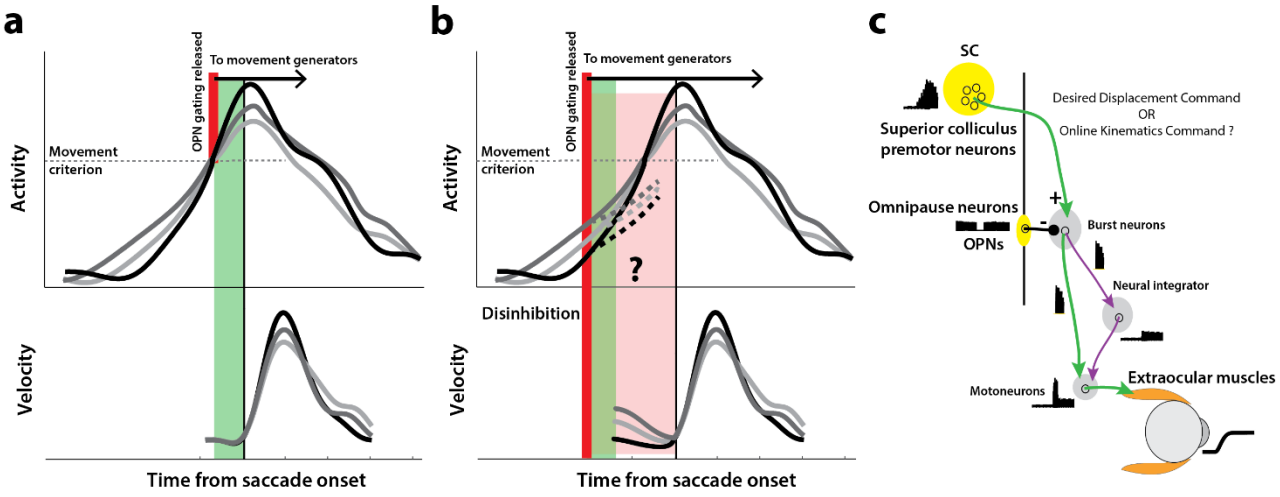

Figure 1. Conceptual schematic of saccade and pre-saccade motor potential revealed by disinhibition. a. Under normal conditions, premotor activity accumulates at different rates on different trials (three example traces in top row) to a movement initiation criterion, opening downstream gating (thick red line) and triggering the saccade following an efferent delay (~20 ms, green window). Following saccade onset, variation in neural activity is correlated with variation in saccade velocity (match gray scale in top and bottom rows), indicating the neuron's motor potential. **b.** Removal of inhibition through an experimental manipulation at an earlier time (thick red line), during saccade preparation and before the typical movement criterion is reached. The disinhibition may reveal the motor potential of ongoing activity in the form of correlated kinematics of the eye before onset of the actual saccade (light red region, velocity traces in bottom row), and also allows us to study any changes in the dynamics of activity leading up to the reduced latency saccades (dashed activity traces in top row). **c.** Schematic of the premotor circuitry involved in saccade generation. A desired displacement command (or, as tested here, a kinematics-driving command) is sent from neurons in SC to the burst neurons in the brainstem reticular formation (also referred to as the burst generator). This pathway is gated by tonic inhibition from the OPNs under normal conditions. Approximately 20 ms before saccade onset, OPN activity pauses, disinhibiting the burst neurons and allowing the excitatory pathway (green arrows) to actuate an eye movement. This study tests whether disinhibiting the pathway downstream of SC by blink-induced suppression of OPNs results in an immediate eye movement.

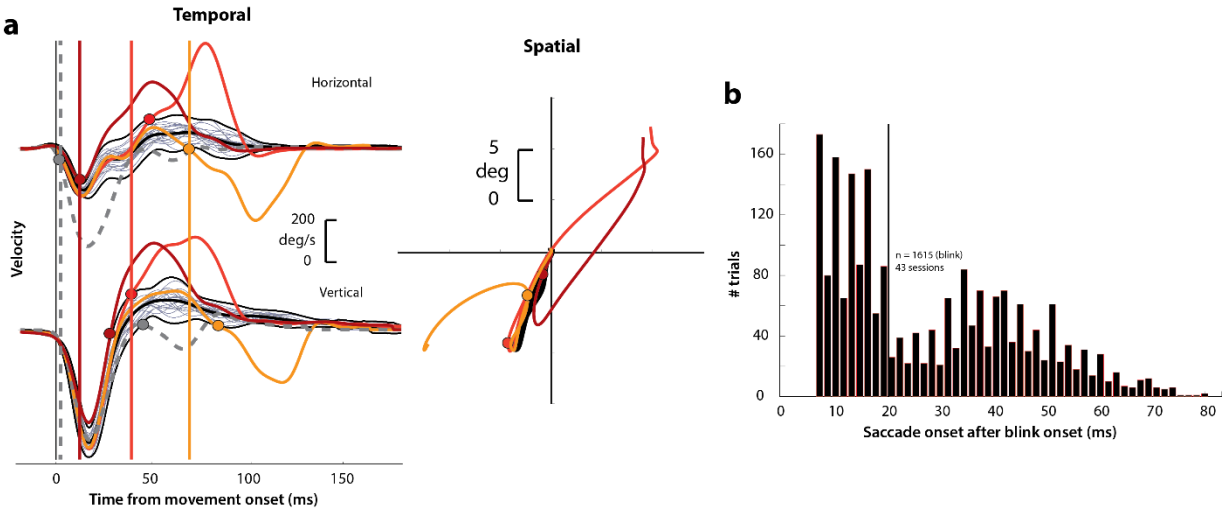

Figure 2. Determining goal-directed saccade onset in blink-triggered eye movements. a. Left column: horizontal (top row) and vertical (bottom row) eye velocity profiles during blink-related eye movements obtained during fixation (BREMs, thin gray traces) and three example blink-triggered saccadic eye movements (colored traces) from one session. The thick black trace in the middle of the BREM profiles is their mean and the two black traces above and below it are ± 2.5 s.d. bounds. Saccade onset was determined to be the point where an individual velocity profile (colored traces) crossed the BREM bounds and stayed outside for 15 consecutive time points. This point was determined independently for the horizontal and vertical channels (colored circles corresponding to each trace in the two rows), and the earlier time point was taken as the onset of the overall movement (vertical colored lines). The dashed gray velocity profile that deviates from the BREM very close to movement onset (<5 ms) is shown to highlight a case where the saccade starts before being perturbed by the blink, and was not considered as a blink-triggered movement in this study. Right column: Spatial trajectories of the eye for the three example blink-triggered movements from the left column, with the corresponding saccade onset time points indicated by the circles. The trajectory of the BREM template is shown in black (for the sake of clarity, only the mean is shown). Note that the movements in this session were made to one of two possible targets on any given trial. **b.** Distribution of goal-directed saccade onset times relative to overall movement onset for blink-triggered movements (n = 1615) across all sessions (n = 43). For the motor potential and accumulation rate analyses (Figures 4-5 and 7), we only considered movements where the blink-triggered saccade started at least 20 ms after overall movement onset (to the right of the vertical line). For the threshold analysis (Figure 6), we considered all blink-triggered movements.

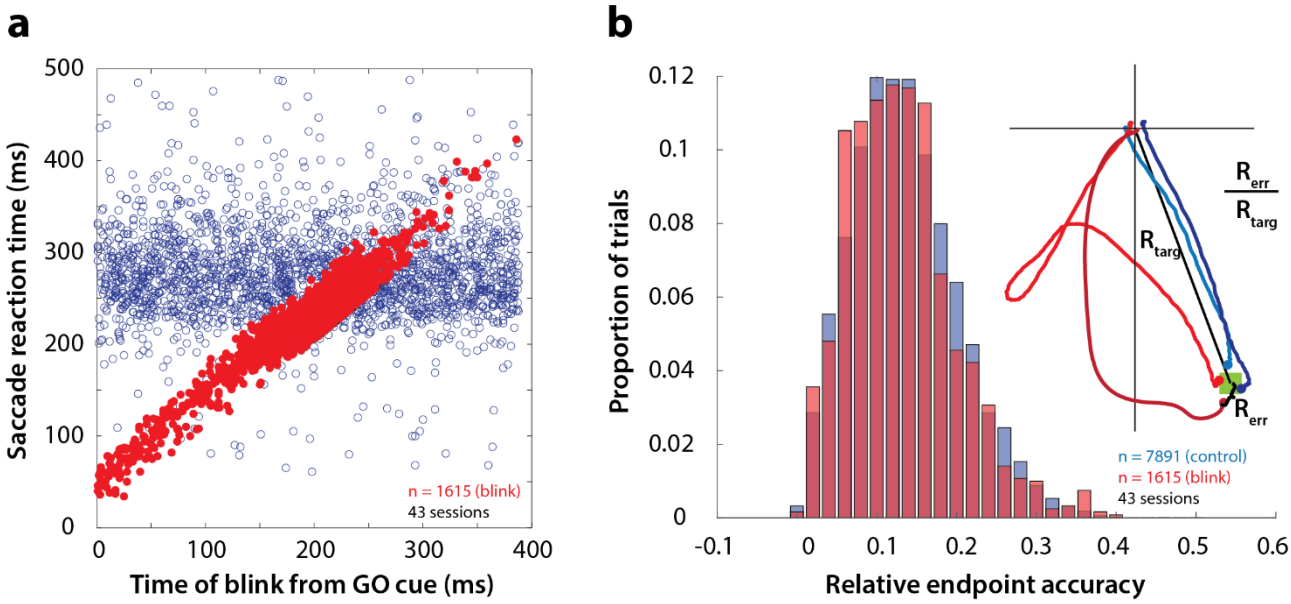

Figure 3. Time course and accuracy of blink-triggered saccades. a. Saccade reaction time as a function of blink onset time across all trials (n = 7891 control trials, 1615 blink trials) and sessions (n = 43). Red filled circles are individual blink trials, and blue circles are from control trials with randomly assigned blink times for comparison. For visualization alone, only a random selection of control trials equal in number to blink trials are plotted. **b.** Endpoint accuracy for control and blink-triggered movements (blue and red histograms, respectively) across all trials from all sessions. To enable comparison across movement amplitudes, the endpoint error was normalized as the actual Euclidean endpoint error from the target divided by the eccentricity of the target, as depicted in the spatial plot in the inset.

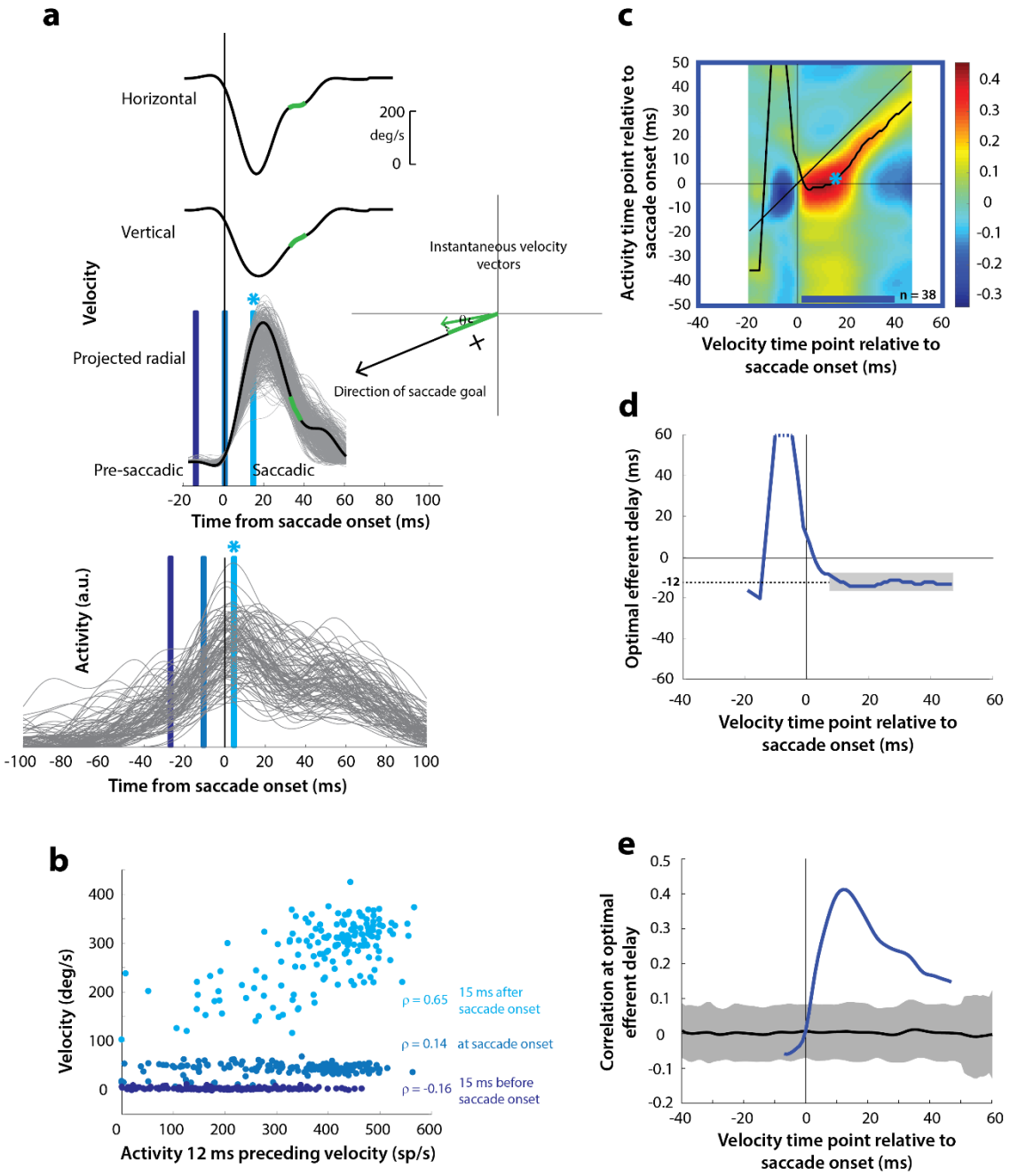

Figure 4. Motor potential during control saccades. a. Estimating motor potential as correlation between neural activity and saccade kinematics. Horizontal and vertical velocity traces (top two rows) on control trials are converted to radial velocity (third row) in the direction of the saccade goal. The projection of the green vector in the inset and the corresponding green parts of the velocity traces illustrate this computation. One trial (thick black trace) is highlighted for clarity. For control trials, the projected and executed vectors are very similar. The bottom row shows neural activity traces on different trials for the neuron recorded in this example session. **b.** Motor potential is estimated as the correlation between neural activity and projected saccade kinematics. The scatter plot of the projected radial velocity 15 ms after saccade onset, at saccade onset, and 15 ms before saccade onset (light, medium, and dark blue

844 points, respectively, and corresponding vertical lines in panel a) against neural activity 12 ms preceding
845 the velocity time points shows that the neuron has motor potential once the saccade has started (Pearson's
846 correlation coefficient = 0.65). Each point corresponds to one trial. **c.** Point-by-point correlation between
847 velocity and activity, averaged across neurons. Heat map colors represent correlation values. As an
848 example, the light blue asterisk refers to the correlation between the velocity and activity corresponding to
849 the time points with the asterisk in panel a. The black curve traces the contour of the highest correlation
850 time points in the activity for each point during the movement. The blue bar at the bottom of the heatmap
851 indicates timepoints at which the average correlation was significant (based on $\pm$ 95% CI from panel e).
852 **d.** Optimal efferent delay computed as the distance of the black trace in panel c from the unity line.
853 Negative values for the delay are causal, i.e., correlation was high for activity points leading the velocity
854 points. The shaded gray bar shows that the optimal delay was consistent during the movement (mean for
855 shaded region = -12 ms) **e.** Population average correlation as a function of time at the -12 ms estimated
856 efferent delay. The black trace is the mean and the gray region is the $\pm$ 95% confidence interval for the
857 bootstrapped (trial-shuffled) correlation distribution.

858

859

860

861

862

863

864

865

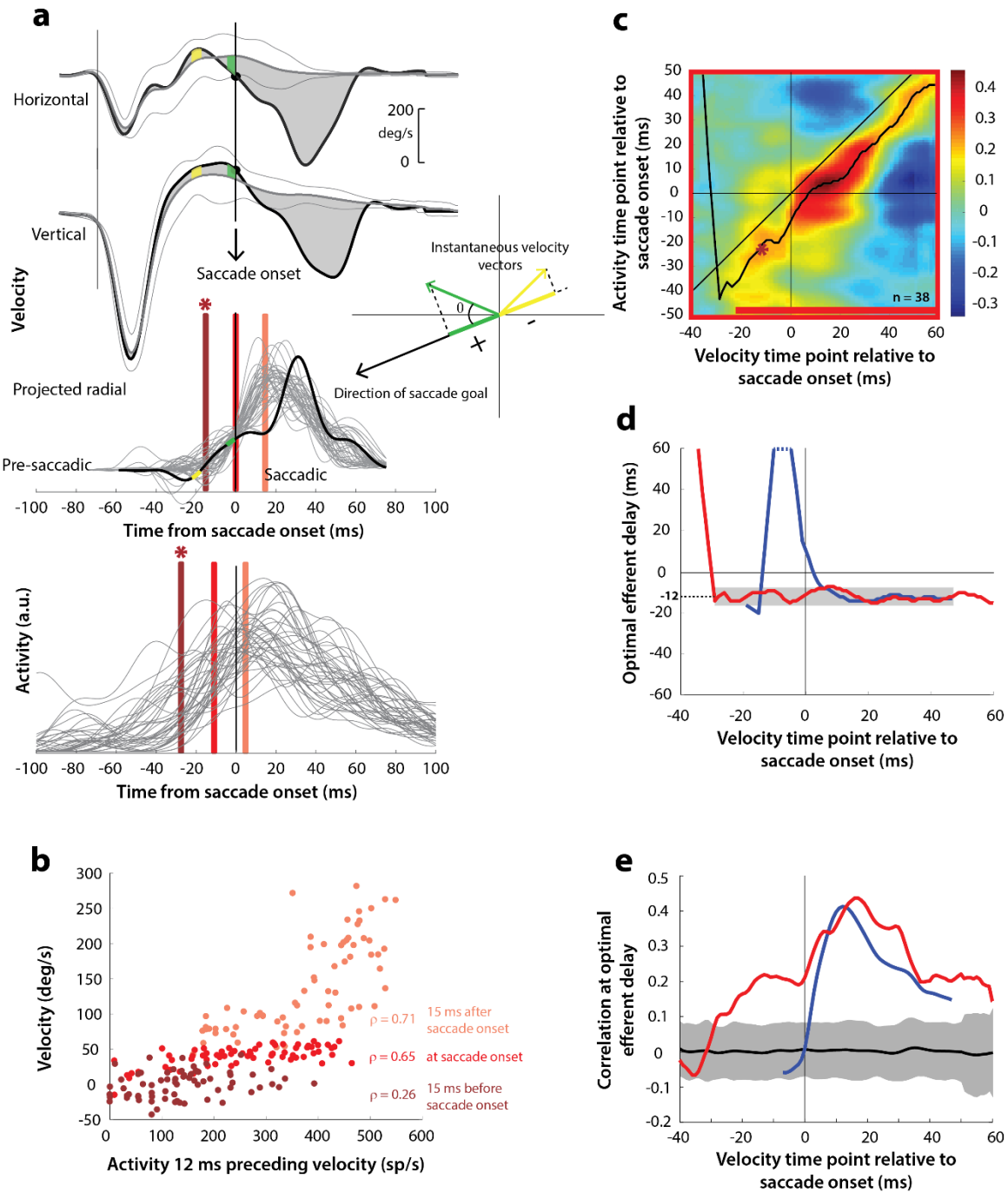

Figure 5. Motor potential on blink trials. a. Computation of the kinematic variable for blink-triggered movements. Horizontal and vertical velocities (thick black traces in top two rows) are converted to residual velocities (gray fill) after subtracting the corresponding mean BREM template (middle thin black trace in top two rows), in order to discount the effects of intrinsic variability in the BREM itself. The radial residual velocity (third row) in the direction of the saccade goal is then computed, similar to Figure 4a. The green and yellow time points in the velocity traces (shown as thicker than an instant for clarity), represented as corresponding velocity vectors in the inset, illustrate this process. For example, the green velocity residual, immediately before saccade onset, deviates negatively from the BREM in the horizontal

component, and positively in the vertical component, resulting in an instantaneous kinematic vector pointing leftwards and upwards. The component of this vector in the direction of the saccade goal is then taken as the kinematic variable for this time point (also compare Supplementary Figure 2). **b.** Scatter plot of the neural activity versus velocity at the three indicated time points (red points of various saturation, at corresponding red lines in panel a) for blink-triggered movements. As in Figure 4b, these are plotted at the -12 ms shift between activity and velocity Note the strong correlation for pre-saccade time points compared to Figure 4b. **c.** Point-by-point correlation of projected residual velocity with activity, averaged across neurons, for blink-triggered movements. The velocity time points are with respect to time of saccade onset extracted from the blink-triggered movement. The dark red asterisk points to the correlation between the velocity and activity corresponding to the time points with the asterisk in panel a. The black curve traces the contour of the highest correlation time points in the activity for each point during the movement. The red bar at the bottom of the heatmap indicates timepoints at which the average correlation was significant (based on $\pm$ 95% CI from panel e). **d.** Optimal efferent delay computed as the distance of the black trace in panel c from the unity line. The red trace is for blink-triggered movements, and the blue trace is from Figure 4d for control saccades, overlaid for comparison. Negative values for the delay are causal, i.e., correlation was high for activity points leading the velocity points. The gray bar highlights the fact that the optimal delay was consistent during both control and blink-triggered saccades, and both before and after saccade onset for the latter (mean for shaded region = -12 ms). **e.** Population average correlation for blink-triggered movements (red trace) as a function of time at the -12 ms estimated efferent delay. The blue trace is from Figure 4e for control saccades, overlaid for comparison. The black trace is the mean and the gray region is the $\pm$ 95% confidence interval for the bootstrapped (trial-shuffled) correlation distribution.

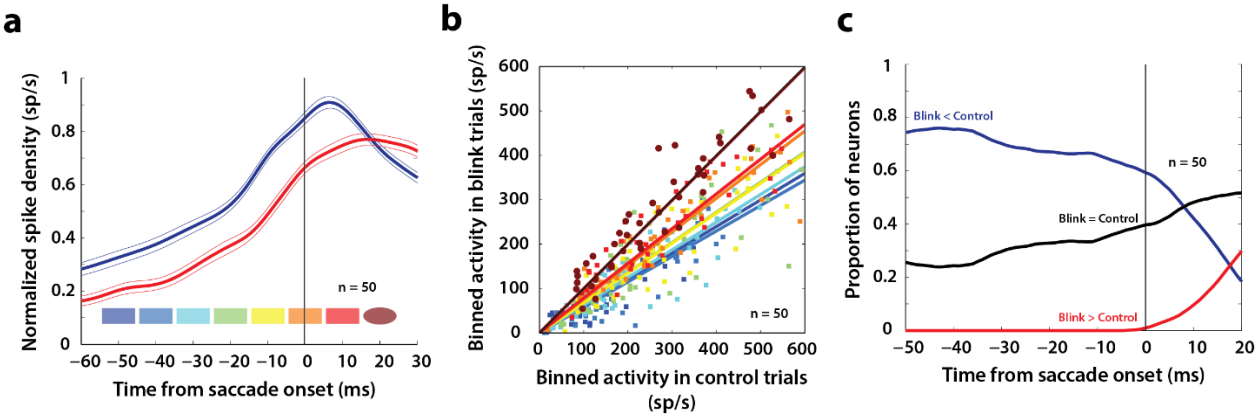

Figure 6. Analysis of putative threshold. a. Average normalized population activity (thick traces) aligned on saccade onset for control (blue trace) and blink (red trace) trials. The thin lines represent s.e.m. The colored swatches at the bottom show the time windows used for the analysis presented in **b**; their shapes represent the presence (rectangle) or absence (ellipse) of a significant difference between control and blink rates in that time window. **b.** Scatter plot of the activities of individual neurons (n=50) in the time windows illustrated in **a** for control versus blink trials (each set of colored points corresponds to one time window). Square points indicate that the activity in control trials was higher in that window compared to blink trials, and circles indicate that there was no significant difference between the two conditions. Colored lines indicate linear fits to the scatter at the corresponding time window. The diagonal (thin black line) is the unity line; it overlaps with the dark brown line. **c.** Proportion of neurons exhibiting the corresponding labelled differences between the two conditions as a function of time.

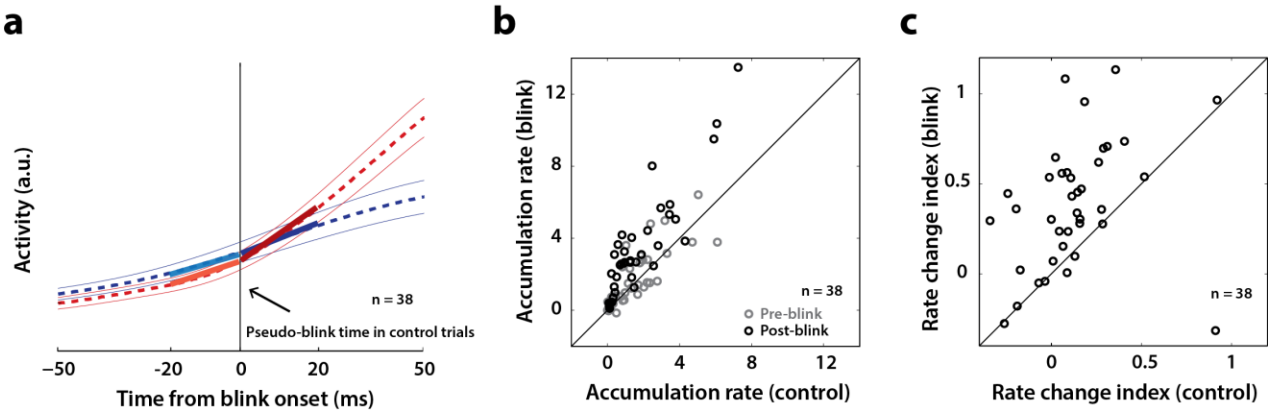

Figure 7. Analysis of accumulation rate change following perturbation. a. Schematic illustrating the computation of accumulation rates before and after the blink. The snippet shows the average population activity (dashed lines) ± s.e.m (thin lines) centered on blink onset for blink trials (red trace) and pseudo-blink onset from the surrogate dataset for control trials (blue trace). The thick lines represent linear fits to the activity 20 ms before (lighter colors) and after (dark colors) the blink time. **b.** Scatter plot of pre-blink (gray circles) and post-blink (black circles) accumulation rates (slopes of fits shown in panel a) of individual neurons for control versus blink trials. The unity line is on the diagonal. **c.** Scatter plot of the pre-to-post rate modulation index $\frac{rate_{post}-rate_{pre}}{rate_{post}+rate_{pre}}$ for control versus blink trials.

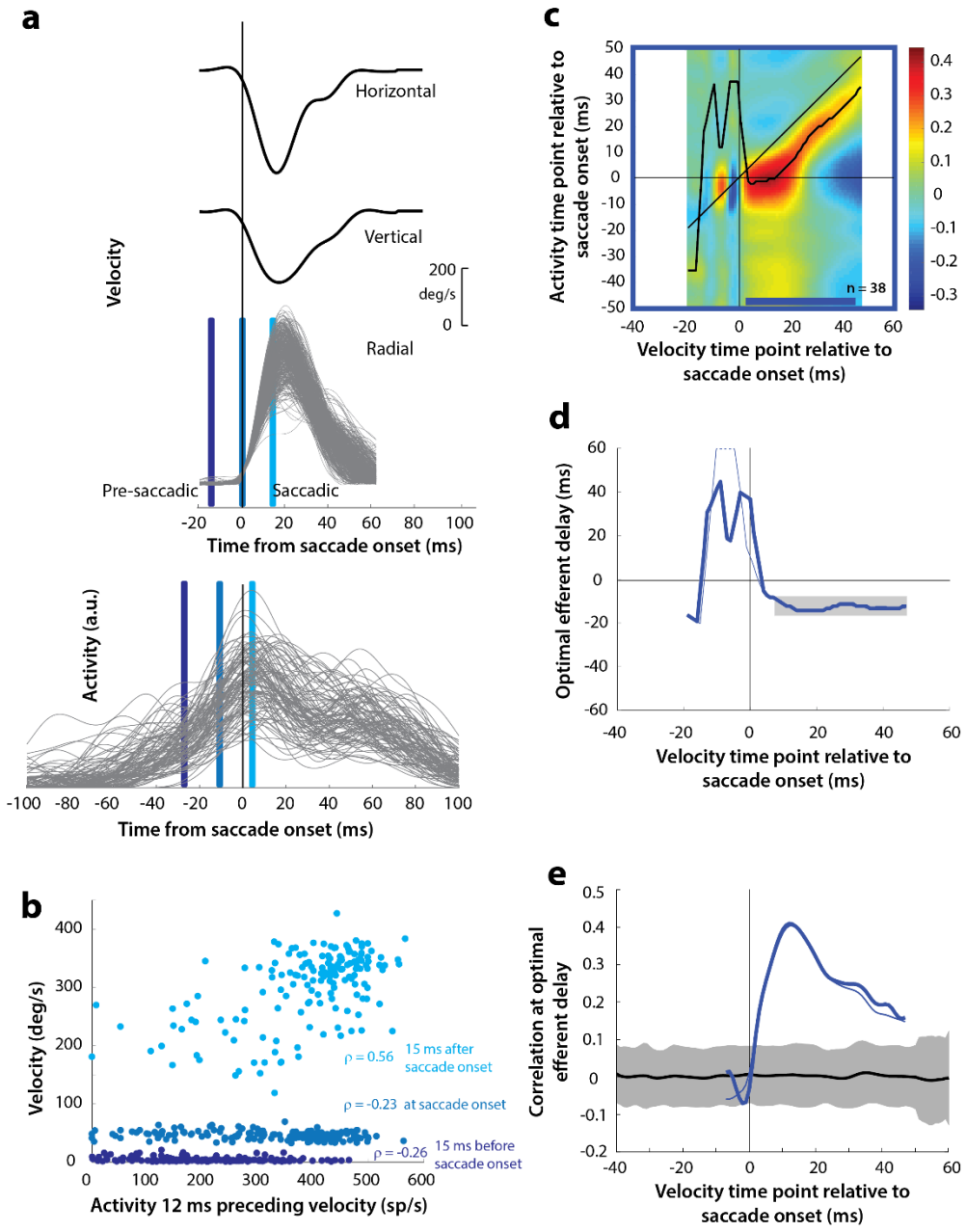

Supplementary Figure 1. Motor potential during control saccades, computed with raw velocities. a. As in Figure 4a, horizontal and vertical velocity traces (top two rows) on control trials are converted to radial velocity (third row). In contrast to Figure 4a, the velocities are used *as is* to compute motor potential, without projecting onto the direction of the saccade goal. The bottom row shows neural activity traces on different trials for the neuron recorded in this example session (same as Figure 4a). **b.** Motor potential is estimated as the correlation between neural activity and saccade kinematics in appropriate time windows. The scatter plot of the projected radial velocity 15 ms after saccade onset, at saccade onset, and 15 ms before saccade onset (light, medium, and dark blue points, respectively, and corresponding vertical lines in panel a) against neural activity 12 ms preceding the velocity time points. Each point corresponds to one trial. **c.** Point-by-point correlation of velocity and activity, averaged across neurons.

953 The black curve traces the contour of the highest correlation time points in the activity for each point
954 during the movement. The blue bar at the bottom of the heatmap indicates timepoints at which the
955 average correlation was significant (based on ± 95% CI from panel e). **d.** Optimal efferent delay (thick
956 blue trace) computed as the distance of the black trace in panel c from the unity line. Negative values for
957 the delay are causal, i.e., correlation was high for activity points leading the velocity points. The gray bar
958 shows that the optimal delay was consistent during the movement (-12 ms) **e.** Population average
959 correlation as a function of time at the -12 ms estimated efferent delay. The black trace is the mean and
960 the gray region is the ± 95% confidence interval for the bootstrapped (trial-shuffled) correlation
961 distribution. The thin traces in panels d-e are from Figures 4d-e, overlaid for comparison.

962

963

964

965

966

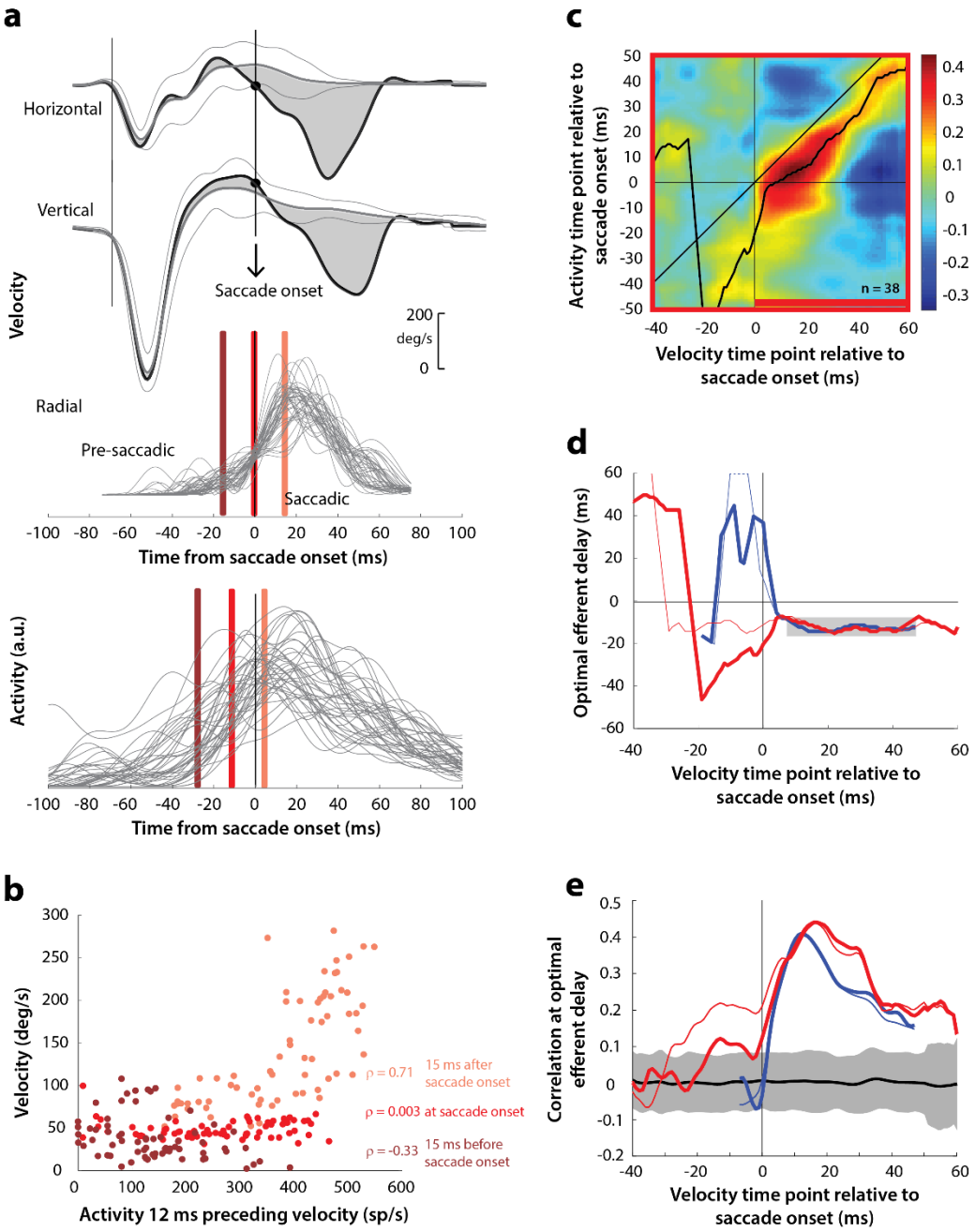

Supplementary Figure 2. Motor potential on blink trials, computed with raw velocities. a. As in Figure 5a, horizontal and vertical velocity traces (top two rows) during blink-triggered movements are converted to radial velocity (third row). In contrast to Figure 5a, the residual velocities (gray shaded deviation from the BREM template) are used *as is* to compute motor potential, without projecting onto the direction of the saccade goal. The bottom row shows neural activity traces on different trials for the neuron recorded in this example session (same as Figure 5a). **b.** Scatter plot of the neural activity versus velocity at the three time points (shaded red windows) from panel a for blink-triggered movements. **c.** Point-by-point correlation of velocity and activity, averaged across neurons, for blink-triggered movements. The velocity time points are with respect to time of saccade onset extracted from the blink-

triggered movement. The black curve traces the contour of the highest correlation time points in the activity for each point during the movement. The red bar at the bottom of the heatmap indicates timepoints at which the average correlation was significant (based on ± 95% CI from panel e). **d.** Optimal efferent delay computed as the distance of the black trace in panel c from the unity line. The thick red trace is for blink-triggered movements computing using raw kinematics, and the others are from previous analyses overlaid for comparison (thin red trace is from Figure 5d, thick blue trace is from Supplementary Figure 1d, and thin blue trace is from Figure 4d). Negative values for the delay are causal, i.e., correlation was high for activity points leading the velocity points. The estimated efferent delay after saccade onset was consistent with the result in Figure 5 (mean for shaded region = -12 ms), but note the abrupt deviation from this value in the pre-saccade period, compared to the thin red trace. **e.** Population average correlation for blink-triggered movements (thick red trace) as a function of time at the -12 ms estimated efferent delay. As in panel d, the other traces are from previous analyses, overlaid for comparison. The black trace is the mean and the gray region is the ± 95% confidence interval for the bootstrapped (trial-shuffled) correlation distribution.

References

Afshar A, Santhanam G, Yu BM, Ryu SI, Sahani M, Shenoy KV (2011) Single-trial neural correlates of arm movement preparation. Neuron 71:555-564.

Arai K, Keller EL, Edelman JA (1994) Two-dimensional neural network model of the primate saccadic system. Neural Networks 7:1115-1135.

Balan PF, Ferrera VP (2003) Effects of gaze shifts on maintenance of spatial memory in macaque frontal eye field. J Neurosci 23:5446-5454.

Bryant CL, Gandhi NJ (2005) Real-time data acquisition and control system for the measurement of motor and neural data. J Neurosci Methods 142:193-200.

Buonocore A, Chen CY, Tian X, Idrees S, Munch TA, Hafed ZM (2017) Alteration of the microsaccadic velocity-amplitude main sequence relationship after visual transients: implications for models of saccade control. J Neurophysiol 117:1894-1910.

Card G, Dickinson MH (2008) Visually mediated motor planning in the escape response of Drosophila. Curr Biol 18:1300-1307.

Carello CD, Krauzlis RJ (2004) Manipulating intent: evidence for a causal role of the superior colliculus in target selection. Neuron 43:575-583.

Carpenter RH, Williams ML (1995) Neural computation of log likelihood in control of saccadic eye movements [see comments]. Nature 377:59-62.

Churchland MM, Santhanam G, Shenoy KV (2006a) Preparatory activity in premotor and motor cortex reflects the speed of the upcoming reach. J Neurophysiol 96:3130-3146.

Churchland MM, Yu BM, Ryu SI, Santhanam G, Shenoy KV (2006b) Neural variability in premotor cortex provides a signature of motor preparation. J Neurosci 26:3697-3712.

Churchland MM, Cunningham JP, Kaufman MT, Foster JD, Nuyujukian P, Ryu SI, Shenoy KV (2012) Neural population dynamics during reaching. Nature 487:51-56.

Cisek P, Puskas GA, El-Murr S (2009) Decisions in changing conditions: the urgency-gating model. J Neurosci 29:11560-11571.

Cohen B, Henn V (1972) Unit activity in the pontine reticular formation associated with eye movements. Brain Res 46:403-410.

Corneil BD, Munoz DP (2014) Overt responses during covert orienting. Neuron 82:1230-1243.

Corneil BD, Olivier E, Munoz DP (2004) Visual responses on neck muscles reveal selective gating that prevents express saccades. Neuron 42:831-841.

Cullen KE, Guitton D (1997) Analysis of primate IBN spike trains using system identification techniques. I. Relationship To eye movement dynamics during head-fixed saccades. J Neurophysiol 78:3259-3282.

Dorris MC, Paré M, Munoz DP (1997) Neuronal activity in monkey superior colliculus related to the initiation of saccadic eye movements. J Neurosci 17:8566-8579.

Elsayed GF, Lara AH, Kaufman MT, Churchland MM, Cunningham JP (2016) Reorganization between preparatory and movement population responses in motor cortex. Nat Commun 7:13239.

Fotowat H, Gabbiani F (2007) Relationship between the phases of sensory and motor activity during a looming-evoked multistage escape behavior. J Neurosci 27:10047-10059.

Gandhi NJ, Bonadonna DK (2005) Temporal interactions of air-puff evoked blinks and saccadic eye movements: Insights into motor preparation. J Neurophysiol 93:1718-1729.

Gandhi NJ, Katnani HA (2011a) Motor functions of the superior colliculus. Annu Rev Neurosci 34:203-229.

Gandhi NJ, Katnani HA (2011b) Interactions of eye and eyelid movements. In: Oxford Handbook of Eye Movements (Liversedge SP, Gilchrist ID, Everling S, eds), pp 323-338. New York: Oxford University Press.

Gold JI, Shadlen MN (2000) Representation of a perceptual decision in developing oculomotor commands. Nature 404:390-394.

1062 Goldberg ME, Wurtz RH (1972) Activity of superior colliculus in behaving monkey. II. Effect of
1063 attention on neuronal responses. J Neurophysiol 35:560-574.
1064 Goossens HH, Van Opstal AJ (2000a) Blink-perturbed saccades in monkey. II. Superior colliculus
1065 activity. J Neurophysiol 83:3430-3452.
1066 Goossens HH, Van Opstal AJ (2000b) Blink-perturbed saccades in monkey. I. Behavioral analysis. J
1067 Neurophysiol 83:3411-3429.
1068 Goossens HH, Van Opstal AJ (2006) Dynamic ensemble coding of saccades in the monkey superior
1069 colliculus. J Neurophysiol 95:2326-2341.
1070 Haith AM, Pakpoor J, Krakauer JW (2016) Independence of Movement Preparation and Movement
1071 Initiation. J Neurosci 36:3007-3015.
1072 Hanes DP, Schall JD (1996) Neural control of voluntary movement initiation. Science 274:427-430.
1073 Hanks T, Kiani R, Shadlen MN (2014) A neural mechanism of speed-accuracy tradeoff in macaque area
1074 LIP. Elife 3.
1075 Heitz RP, Schall JD (2012) Neural mechanisms of speed-accuracy tradeoff. Neuron 76:616-628.
1076 Hikosaka O, Nakamura K, Nakahara H (2006) Basal ganglia orient eyes to reward. J Neurophysiol
1077 95:567-584.
1078 Hoffman JE, Subramaniam B (1995) The role of visual attention in saccadic eye movements. Percept
1079 Psychophys 57:787-795.
1080 Horwitz GD, Newsome WT (1999) Separate signals for target selection and movement specification in
1081 the superior colliculus. Science 284:1158-1161.
1082 Ignashchenkova A, Dicke PW, Haarmeier T, Thier P (2004) Neuron-specific contribution of the superior
1083 colliculus to overt and covert shifts of attention. Nature neuroscience 7:56-64.
1084 Jagadisan UK, Gandhi NJ (2016) Disruption of Fixation Reveals Latent Sensorimotor Processes in the
1085 Superior Colliculus. J Neurosci 36:6129-6140.
1086 Jantz JJ, Watanabe M, Everling S, Munoz DP (2013) Threshold mechanism for saccade initiation in the
1087 frontal eye field and superior colliculus. J Neurophysiol 109:2767-2780.
1088 Joo SJ, Katz LN, Huk AC (2016) Decision-related perturbations of decision-irrelevant eye movements.
1089 Proceedings of the National Academy of Sciences of the United States of America 113:1925-
1090 1930.
1091 Juan CH, Shorter-Jacobi SM, Schall JD (2004) Dissociation of spatial attention and saccade preparation.
1092 Proceedings of the National Academy of Sciences of the United States of America 101:15541-
1093 15544.
1094 Katnani HA, Gandhi NJ (2013) Time course of motor preparation during visual search with flexible
1095 stimulus-response association. J Neurosci 33:10057-10065.
1096 Kaufman MT, Churchland MM, Ryu SI, Shenoy KV (2014) Cortical activity in the null space: permitting
1097 preparation without movement. Nature neuroscience 17:440-448.
1098 Kaufman MT, Seely JS, Sussillo D, Ryu SI, Shenoy KV, Churchland MM (2016) The Largest Response
1099 Component in the Motor Cortex Reflects Movement Timing but Not Movement Type. eNeuro 3.
1100 Keller EL (1974) Participation of medial pontine reticular formation in eye movement generation in
1101 monkey. J Neurophysiol 37:316-332.
1102 Lo CC, Wang XJ (2006) Cortico-basal ganglia circuit mechanism for a decision threshold in reaction time
1103 tasks. Nature neuroscience 9:956-963.
1104 McPeek RM, Keller EL (2002) Saccade target selection in the superior colliculus during a visual search
1105 task. J Neurophysiol 88:2019-2034.
1106 Miyashita N, Hikosaka O (1996) Minimal synaptic delay in the saccadic output pathway of the superior
1107 colliculus studied in awake monkey. Experimental brain research 112:187-196.
1108 Moore T, Armstrong KM (2003) Selective gating of visual signals by microstimulation of frontal cortex.
1109 Nature 421:370-373.
1110 Nakagawa H, Nishida Y (2012) Motor planning modulates sensory-motor control of collision avoidance
1111 behavior in the bullfrog, Rana catesbeiana. Biol Open 1:1094-1101.

Newsome WT, Britten KH, Movshon JA (1989) Neuronal correlates of a perceptual decision. Nature 341:52-54.

Paré M, Munoz DP (1996) Saccadic reaction time in the monkey: advanced preparation of oculomotor programs is primarily responsible for express saccade occurrence. J Neurophysiol 76:3666-3681.

Paré M, Hanes DP (2003) Controlled movement processing: superior colliculus activity associated with countermanded saccades. J Neurosci 23:6480-6489.

Platt ML, Glimcher PW (1999) Neural correlates of decision variables in parietal cortex. Nature 400:233-238.

Preuss T, Osei-Bonsu PE, Weiss SA, Wang C, Faber DS (2006) Neural representation of object approach in a decision-making motor circuit. J Neurosci 26:3454-3464.

Ramakrishnan A, Murthy A (2013) Brain mechanisms controlling decision making and motor planning. Prog Brain Res 202:321-345.

Ratcliff R, Rouder JN (1998) Modeling response times for two-choice decisions. Psychol Rev 9:347-356.

Rizzolatti G, Riggio L, Dascola I, Umilta C (1987) Reorienting attention across the horizontal and vertical meridians: evidence in favor of a premotor theory of attention. Neuropsychologia 25:31-40.

Rodgers CK, Munoz DP, Scott SH, Pare M (2006) Discharge properties of monkey tectoreticular neurons. J Neurophysiol 95:3502-3511.

Rottach KG, Das VE, Wohlgemuth W, Zivotofsky AZ, Leigh RJ (1998) Properties of horizontal saccades accompanied by blinks. J Neurophysiol 79:2895-2902.

Salinas E, Scerra VE, Hauser CK, Costello MG, Stanford TR (2014) Decoupling speed and accuracy in an urgent decision-making task reveals multiple contributions to their trade-off. Front Neurosci 8:85.

Schall JD, Hanes DP (1993) Neural basis of saccade target selection in frontal eye field during visual search. Nature 366:467-469.

Schall JD, Purcell BA, Heitz RP, Logan GD, Palmeri TJ (2011) Neural mechanisms of saccade target selection: gated accumulator model of the visual-motor cascade. Eur J Neurosci 33:1991-2002.

Schultz KP, Williams CR, Busettini C (2010) Macaque pontine omnipause neurons play no direct role in the generation of eye blinks. J Neurophysiol 103:2255-2274.

Segraves MA (1992) Activity of monkey frontal eye field neurons projecting to oculomotor regions of the pons. J Neurophysiol 68:1967-1985.

Servant M, White C, Montagnini A, Burle B (2015) Using Covert Response Activation to Test Latent Assumptions of Formal Decision-Making Models in Humans. J Neurosci 35:10371-10385.

Sommer MA, Wurtz RH (2001) Frontal eye field sends delay activity related to movement, memory, and vision to the superior colliculus. J Neurophysiol 85:1673-1685.

Sylvestre PA, Cullen KE (2006) Premotor correlates of integrated feedback control for eye-head gaze shifts. J Neurosci 26:4922-4929.

Thompson KG, Biscoe KL, Sato TR (2005) Neuronal basis of covert spatial attention in the frontal eye field. J Neurosci 25:9479-9487.

Thompson KG, Hanes DP, Bichot NP, Schall JD (1996) Perceptual and motor processing stages identified in the activity of macaque frontal eye field neurons during visual search. J Neurophysiol 76:4040-4055.

Thura D, Beauregard-Racine J, Fradet CW, Cisek P (2012) Decision making by urgency gating: theory and experimental support. J Neurophysiol 108:2912-2930.

Usher M, McClelland JL (2001) The time course of perceptual choice: the leaky, competing accumulator model. Psychol Rev 108:550-592.

Valls-Sole J, Sole A, Valldeoriola F, Munoz E, Gonzalez LE, Tolosa ES (1995) Reaction time and acoustic startle in normal human subjects. Neuroscience letters 195:97-100.

Van Gisbergen JA, Van Opstal AJ, Tax AA (1987) Collicular ensemble coding of saccades based on vector summation. Neuroscience 21:541-555.

Walton MM, Gandhi NJ (2006) Behavioral evaluation of movement cancellation. J Neurophysiol 96:2011-2024.

1163 Wurtz RH, Sommer MA, Paré M, Ferraina S (2001) Signal transformations from cerebral cortex to
1164 superior colliculus for the generation of saccades. Vision Res 41:3399-3412.
1165 Zandbelt B, Purcell BA, Palmeri TJ, Logan GD, Schall JD (2014) Response times from ensembles of
1166 accumulators. Proceedings of the National Academy of Sciences of the United States of America
1167 111:2848-2853.

1168